

A Hamiltonian approach for point vortices on non-orientable surfaces I: the Möbius band

Nataliya A. Balabanova, James Montaldi

February 15, 2022

Abstract

This is the first of two companion papers, in which we investigate vortex motion on non-orientable two dimensional surfaces. We establish the ‘Hamiltonian’ approach to point vortex motion on non-orientable surfaces through describing the phase space, the Hamiltonian and the local equations of motion. This paper is primarily focused on the dynamics on the Möbius band. To this end, we adapt some of the known notions of vortex dynamics to non-orientable surfaces. We write Hamiltonian-type equations of vortex motion explicitly and follow that by the description of relative equilibria and a thorough investigation of motion of one and two vortices, with emphasis on the periodicity of motion.

Contents

1	Introduction	2
2	Hamiltonian approach to point vortex flows on non-orientable manifolds	5
2.1	Twisted scalars and vector fields	5
2.2	Vorticity and vortex strength	6
2.3	Phase space for point vortices	6
2.4	The Hamiltonian	8
2.5	The momentum map	10
3	Vortex motion on a Möbius band	11
3.1	Equations of motion	12
3.2	Invariants and relative equilibria	13
3.3	A general class of equilibria	13
3.4	The N-ring relative equilibria	14
3.5	Motion of a single vortex	15
4	Motion of two vortices	16
4.1	Fixed equilibria	18
4.2	General motion of two vortices	19
4.2.1	Zero momentum	24
4.2.2	$\Gamma_1 = \Gamma_2$	25
5	Concluding remarks	26

A Velocity of the N-ring relative equilibria 26

References 29

1 Introduction

Neither of the classical approaches to fluid dynamics prohibits considering fluid motion on non-orientable manifolds: the Euler equations

$$\rho \frac{Dv}{Dt} = -\nabla p$$

with ρ the density, p the pressure and v the divergence free flow of the fluid only demand that the manifold in question be Riemannian (see [19]); secondly, Arnold's interpretation [6] of the fluid flow as diffeomorphisms that preserve the volume element is a construction defined in the non-orientable case as well. On the other hand, the definition of vorticity does depend on a choice of orientation, so the equation for the vorticity is only well-defined if the manifold is oriented.

Much has been written about point vortices on a general (oriented) surface (see [2, 4, 15, 21, 25] and many others), and the setup involves using the strength $\Gamma \in \mathbb{R}$ of each point vortex, the symplectic form on the surface and the Hamiltonian which involves the hydrodynamic Green's function. The strength of a point vortex is positive if the local direction of flow agrees with the orientation of the surface, and is negative otherwise. The symplectic form defines the orientation of the surface.

This is the first of two works (see [7] for the second) describing how to adapt the Hamiltonian approach to point vortices to non-orientable surfaces. On such surfaces, the sign of the vortex strength cannot be defined consistently, and neither is there a symplectic form.

To circumvent this, we define the vortex strength as a *twisted* or *pseudo-scalar*, which means that to each local orientation one defines a scalar, and opposite orientations give rise to opposite scalar values. The equations of motion, in turn, will be described locally on oriented charts; however, as we will see below, their form will allow for globally defined trajectories of motion.

A system of N point vortices, of strengths $\Gamma_1, \dots, \Gamma_N$, on an oriented surface M has phase space $M^N \setminus \Delta$ where $M^N = M \times M \times \dots \times M$ and Δ is the big diagonal. The symplectic form is

$$\sigma = \bigoplus_{j=1}^N \Gamma_j \sigma_j \tag{1.1}$$

where σ_j is the symplectic form on the j th copy of M , and the Hamiltonian is equal to the sum

$$\mathcal{H}(x_1, \dots, x_N) = - \sum_{i \neq j} \Gamma_i \Gamma_j G(x_i, x_j) - \frac{1}{2} \sum_j \Gamma_j^2 R(x_j), \tag{1.2}$$

where $G(x, y)$ is the hydrodynamic Green's function and $R(x)$ is the Robin function (see for example [8, 12] and references therein) which is defined by

$$R(x) = \lim_{y \rightarrow x} \left(G(x, y) - \frac{1}{2\pi} \log d(x, y) \right). \tag{1.3}$$

where $d(x, y)$ is the geodesic distance between x and y .

The simplest example of such a system is one on the plane, consisting of the standard planar symplectic form and the logarithmic Hamiltonian $\mathcal{H} = -\frac{1}{2\pi} \sum_{\alpha < \beta} \Gamma_\alpha \Gamma_\beta \log(|z_\alpha - z_\beta|)$ (see [3, 16, 23], etc.).

Imposing specific symmetries on a planar system allows for its interpretation as one on a two dimensional manifold.

For example, dividing the plane into evenly spaced vertical strips of width $2\pi r$, each with the exact same set of point vortices gives us a system on a cylinder (see [5, 22] for detailed construction), with the Hamiltonian given by $\mathcal{H} = -\frac{1}{2\pi} \sum_{k < l} \Gamma_k \Gamma_l \log \left| \sin \frac{z_k - z_l}{2r} \right|$.

Periodic vortex configurations on lattices yield systems on flat tori, the dynamics of which have been studied, for example, in [24, 29]. In [12, 17] and [28] systems on curved tori and spheres are investigated; [26] derives an algorithm determining the motion of a single point vortex on a surface of constant curvature and of genus greater than one. In a more general setup, [27] establishes existence and uniqueness of the Green's function under hydrodynamic conditions at the boundaries and ends of the surface for an oriented Riemannian surface of finite topological type. The Green's function, together with the Robin function, are then used to describe the motion of systems of point vortices.

Certain symmetries of systems of point vortices allow us to descend from an orientable double cover to a non-orientable manifold. The systems with such symmetries have been considered previously, but the option of writing the equations intrinsically on non-orientable manifolds has never, to our knowledge, been addressed.

For instance, [17] studies vortex systems on a sphere with a particular symmetry: vortices come in pairs of opposite strength that lie on the antipodal points on the sphere. Though not explicitly mentioned in the original text, this system is the double cover of one on the projective plane.

In this paper we develop a 'Hamiltonian' approach to point vortex motion on non-orientable surfaces and investigate in detail the case when the non-orientable manifold is the Möbius band.

Hamiltonian approach to point vortex flows on non-orientable manifolds

We establish that for flows on non-orientable manifolds vorticity must be interpreted as a two-form; for point vortex flow it means that its scalar counterpart, point vortex strength Γ , must be a so-called *twisted scalar*. The same interpretation of vorticity and stream function as twisted functions was adopted in [31].

Using the approach to construction of the phase space from [20], we demonstrate that the phase space for the motion of N point vortices on a non-orientable manifold M is the N -fold Cartesian product $\bigotimes_{i=1}^N \widetilde{M}$, where \widetilde{M} is the orientable double cover of M .

We find the explicit form of the Hamiltonian (2.5) and prove that it is a regular (i.e., not twisted) function on M and $\bigotimes_{i=1}^N M$ and is constructed in a standard way from the Green's function of the Laplace operator and its Robin function (Proposition 2.4).

Explicit formulae for the Möbius band

In this section, we restrict our attention to point vortex motion on the Möbius band.

The model of the Möbius band that we employ is an infinite strip of width π on the plane with oppositely oriented vertical sides (as in Figure 1), with a cylinder $\mathbb{C}/2\pi\mathbb{Z}$ as a double

cover. We call the boundary of the strip the *imaginary boundary*.

Since this model induces local orientation, we assume that point vortices move inside the strip as usual, but upon reaching the imaginary boundary they 'jump' to the other side, change the sign of their strength and the sign of their y coordinate.

Periodizing the formulae on the double cover, we are able to write the Hamiltonian and the Hamiltonian type equations of the system; we introduce a *Möbius flip* (formalization of the 'vortex jump' described above and the orientation changing isometric involution for the double cover) of the covering system on a cylinder and prove that the Hamiltonian and the equations of motion are invariant under the Möbius flip, applied to any number of vortices. This guarantees that not only the equations of motion are well-defined, but that it also doesn't matter where we assume the imaginary boundary to be located: the motion will be the same regardless of where we draw it.

Motion of point vortices

Having derived the equations of motion early in Section 3, we observe that the symmetry group of the system is S^1 , acting by horizontal translations; this action has a globally defined momentum map that is a regular (as opposed to twisted) function. In Section 3.3 we show the existence of a general class of 'equatorial' equilibria, and Section 3.4 is dedicated to particular instances of relative equilibria that are aligned and staggered rings of vortices on the Möbius band.

We describe in detail the motion of a single point vortex in Section 3.5. Due to its simplicity, this case allows for a very clear outlook on how the trajectories of the global motion are glued together. Indeed, even in this simple case it becomes clear that the dynamics is not defined on M , but on \widetilde{M} .

For comparison with the planar case, we investigate the motion of two point vortices with opposite strengths, with centres placed with a vertical or horizontal symmetry. The former configuration will be a relative equilibrium and an example of a so-called vortex street ([30]); the trajectories of the system with horizontal symmetry will be closed loops.

The next arrangement we investigate is an asymptotic one: point vortex strengths are assumed to be arbitrary, but the moduli of y -coordinates of both vortices are taken to be infinitely large. The two will then move in horizontal lines, in the same or opposite directions, depending on the strengths of the vortices. However, due to different velocities this motion will not be a relative equilibrium.

In the final section (Section 4), we describe the motion of a pair of arbitrary point vortices, starting with a description of the fixed equilibria of two vortices.

In order to perform the calculations for the system of two point vortices, we observe that this system on a Möbius band lifts to a system of four point vortices on a cylinder, and vice versa: the motion of a system of four point vortices with certain imposed symmetries on a cylinder correspond to that of a pair of vortices on a Möbius band.

Using the first integral of motion and the dependence of the Hamiltonian solely on $x_1 - x_2$, we reduce the system and establish the minimum number of critical points. Numerical calculations point towards existence of two kinds of arrangements of the level sets of the reduced Hamiltonian; we describe the motion of the system corresponding to all principal types of the level sets within each of them.

2 Hamiltonian approach to point vortex flows on non-orientable manifolds

2.1 Twisted scalars and vector fields

As we have mentioned above, several hydrodynamic notions are directly tied to local orientation; we need their counterparts that are well-defined in the non-orientable case in order to describe our system in a Hamiltonian-like manner.

Let M be a manifold, possibly with boundary. Then at (or in a neighbourhood of) each point $p \in M$ there are two possible orientations. If we let (p, o) be a point together with an orientation, then the collection of such pairs forms the orientation bundle over M ,

$$\pi : \widetilde{M} \rightarrow M$$

which we denote $\mathfrak{or}(M)$. The fibre consists of two points, the two orientations of the manifold at that point. The total space \widetilde{M} of $\mathfrak{or}(M)$ is connected if and only if M is non-orientable. Furthermore, it has a tautological orientation: the projection is a local diffeomorphism, so on each sheet one associates the orientation corresponding to that sheet.

The manifold \widetilde{M} is thereby an oriented double cover of M , and for the three principal 2-dimensional cases this is recognizable globally as the sphere as the double cover of the projective plane, the cylinder as the double cover of the Möbius band and the torus as the double cover of the Klein bottle.

Let $\tau : \widetilde{M} \rightarrow \widetilde{M}$ denote the automorphism of $\mathfrak{or}(M)$ that swaps the two points in each fibre; over each point p it acts by reversing the orientation at p (for example, for the projective plane this is the antipodal map on the sphere). Then M is clearly the quotient of this total space by the action of the group generated by τ .

Any real-valued function, differential form or vector field on M lifts to one on \widetilde{M} which is in each case, invariant under τ . Conversely, any such object (scalar field, vector field etc) on \widetilde{M} invariant under τ descends to a similar object on M . We refer to such objects as **regular**.

On the other hand, if application of τ to say a scalar function f on \widetilde{M} changes its sign ($f \circ \tau = -f$), then it is called a **twisted** or **pseudo**-function on M ; the same applies to forms and vector fields. In other words, the object in question depends on the choice of orientation, and changing orientation changes the sign of the object. This is the case for example of the curl of a vector field in \mathbb{R}^3 . (For in-depth discussion of twisted objects we refer the reader to [1, 9, 10].)

Remark 2.1. Twisted functions are often defined as sections of a twisted line bundle on M . The relationship with the approach above is as follows. Let \widetilde{L} be the trivial line bundle on \widetilde{M} . Then $\pi_* \widetilde{L}$ is a rank-2 vector bundle on M whose fibre over $p \in M$ is $\widetilde{L}_{p'} \oplus \widetilde{L}_{p''}$, where $\pi^{-1}(p) = \{p', p''\}$. Now τ induces an action on $\pi_* \widetilde{L}$ by swapping the two summands. We can then decompose $\pi_* \widetilde{L}$ as the sum of two line bundles over M

$$\pi_* \widetilde{L} = L_+ \oplus L_-$$

where sections of L_+ are those sections invariant under τ and sections of L_- are those whose sign is changed by τ . The sections of L_+ correspond to genuine (regular) functions on M , while sections of L_- correspond to twisted functions on M . A similar construction can be made for vector fields or forms, starting from $T\widetilde{M}$ or $T^*\widetilde{M}$ in place of \widetilde{L} . The sections of $(T\widetilde{M})_-$ or $(T^*\widetilde{M})_-$ are respectively twisted vector fields and twisted one forms.

2.2 Vorticity and vortex strength

Consider a divergence-free vector field v on M (tangent to ∂M), and let $\alpha = v^\flat$ denote the corresponding 1-form defined using the Riemannian metric. Then let $\lambda = d\alpha$: this is the **vorticity 2-form**. It is defined independently of any orientation.

On the other hand, the vorticity-as-a-scalar does depend on the orientation and is defined on \widetilde{M} as follows. Since \widetilde{M} is oriented and Riemannian, it has a natural symplectic form we denote by σ . Given the vorticity 2-form λ on M we can lift this to \widetilde{M} , and find a smooth function ω on \widetilde{M} satisfying $\pi^*\lambda = \omega\sigma$. This is the scalar vorticity on \widetilde{M} .

Now $\tau^*\pi^*\lambda = \pi^*\lambda$, while $\tau^*\sigma = -\sigma$, and it follows that $\tau^*\omega = -\omega$, which is to say that the scalar vorticity ω is a *twisted* scalar on M , as we know from the discussion in the introduction. Indeed, the operation passing from λ to ω is the twisted Hodge star operator, which on non-oriented manifolds takes regular p -forms to twisted $(n-p)$ -forms.

The vorticity equation on M or \widetilde{M} is then

$$\lambda_t + L_v\lambda = 0, \quad \text{or} \quad \omega_t + d_v\omega = 0.$$

The first is an equation of 2-forms on M (involving the Lie derivative L_v), while the second is of twisted scalars.

In the classical hydrodynamical approach for a small oriented neighbourhood of the point vortex the *point vortex strength* Γ is the flux of the vorticity through an open surface A bounded by a curve C that encircles the vortex. In our terminology, that will be an integral of the one-form \mathbf{v}^\flat :

$$\Gamma = \oint_C \mathbf{v}^\flat = \int_{\bar{A}} \lambda \tag{2.1}$$

where \bar{A} is the region A inside C with the given orientation. Observe how the sign of Γ depends on the (local) orientation.

An alternative interpretation of point vortex strength on an oriented manifold \widetilde{M} is the coefficient Γ at the Dirac delta function of the vorticity-as-a-scalar of a point vortex.

Analogously, for point vortices on the non-orientable M , $\Gamma\delta(x)$ is a twisted function (or twisted distribution). As we will see below, the 'twistedness' of Γ will be crucial for the equations of motion to be well-defined; therefore, we assume that $\delta(x)$ is a regular 'function' (distribution), while Γ is a twisted scalar (that is, a real number associated to the point vortex whose sign depends on the local orientation chosen).

2.3 Phase space for point vortices

We follow the approach of Marsden and Weinstein [20], and note that this also holds for non-orientable surfaces. Given an initial vorticity 2-form λ on a 2-dimensional Riemannian manifold M , the phase space¹ for the dynamics is

$$\mathcal{O}_\lambda = \{\phi^*\lambda \mid \phi \in \text{SDiff}(M)\},$$

¹Note that if M is oriented then $\text{SDiff}(M)$ is not connected, and it would be more efficient to restrict to $\text{SDiff}(M)_0$, which consists of volume-preserving diffeomorphisms isotopic to the identity; this is possibly what the authors of [20] had in mind.

where $\text{SDiff}(M)$ is the group of volume-preserving diffeomorphisms of M ; this can be interpreted as the coadjoint orbit of $\text{SDiff}(M)$ containing λ . The symplectic form is given by the Kostant-Kirillov-Souriau form,

$$\Omega_\lambda(L_u\lambda, L_v\lambda) = \int_M \lambda(u, v) dA$$

where $u, v \in \mathcal{X}_0(M)$ (divergence-free vector fields), L_u and L_v are the Lie derivatives and dA is the area measure consistent with the metric. This does not require M itself to be oriented or symplectic. For a regular vorticity form, the Hamiltonian is given by the total kinetic energy of the fluid.

The motion of a system of N point vortices on an orientable surface M is determined by the location and strength of the point vortices; the strength here being the (scalar) vorticity concentrated at a point, in the form of delta functions. In this case, it was pointed out in [20] that the phase space \mathcal{O}_λ can be identified with $M \times M \times \cdots \times M \setminus \Delta$ (the product of N copies of M with the collision set removed). The identification is

$$(x_1, \dots, x_N) \mapsto \sum_j \Gamma_j \delta_{x_j} \sigma \quad (2.2)$$

where σ is the symplectic form on M and δ_p is a delta function supported at p . The symplectic form on \mathcal{O}_λ becomes

$$\Omega_\lambda(\mathbf{u}, \mathbf{v}) = \sum_j \Gamma_j \sigma_{x_j}(u_j, v_j)$$

where $u_j, v_j \in T_{x_j}M$.

The Hamiltonian is given by

$$\mathcal{H}(x_1, \dots, x_N) = - \sum_{i < j} \Gamma_i \Gamma_j G(x_i, x_j) - \frac{1}{2} \sum_j \Gamma_j^2 R(x_j). \quad (2.3)$$

Now consider the case where M is non-orientable. Two or three problems arise when adapting the discussion above and we need to employ the twisted construction described above.

Most obviously, since on M the Γ_j are twisted scalars, it is not clear what the first term in the Hamiltonian (2.3) means. Moreover, the phase space \mathcal{O}_λ can no longer be identified with a product of N copies of M . This is because, a given N -tuple of points (x_1, \dots, x_N) does not determine the interaction between the vortices. Indeed, when M is non-orientable, there is a volume preserving diffeomorphism which takes say x_1 back to x_1 by a ‘non-orienting’ loop, which has the effect of reversing the contribution to the vorticity 2-form at the point x_1 .

Thus, in \mathcal{O}_λ there are vorticities supported at the same points, but with any subset of the local vorticity 2-forms reversed. That is, if $\lambda = \sum_j \lambda_{x_j}$ where λ_{x_j} is a delta-function 2-form (a 2-current), then \mathcal{O}_λ also contains $\lambda' = \sum_j (\pm \lambda_{x_j})$ for all choices of signs. This leads to a parametrization of \mathcal{O}_λ by the product of N double covers of M .

Proposition 2.2. *The phase space \mathcal{O}_λ for a system of N point vortices on a non-orientable surface M can be parametrized by $\tilde{M} \times \cdots \times \tilde{M} \setminus \tilde{\Delta}$, where $\tilde{\Delta}$ is the ‘very big diagonal’ consisting of points $(x'_1, \dots, x'_N) \in \tilde{M}^N$ for which $i \neq j \Rightarrow \pi(x'_i) \neq \pi(x'_j)$.*

The parametrization is constructed in the following way. For the vorticity 2-form λ on M , let $\{x_1, \dots, x_N\}$ be the support of λ . For each x in this set let $\pi^{-1}(x) = \{x', \tau(x')\}$ for some $x' \in \widetilde{M}$. The pull-back of λ to \widetilde{M} is a 2-form, and the tautological symplectic form σ allows us to define the vortex strengths Γ at x' and $-\Gamma$ at $\tau(x')$ (we do not assume $\Gamma > 0$, the vorticity will be positive at the point where the orientation agrees with the direction of circulation of the vortex, and negative (of the same magnitude) at the other point). The system can be parametrized by (x'_1, \dots, x'_N) and the associated vorticities $(\Gamma_1, \dots, \Gamma_N)$.

2.4 The Hamiltonian

In the same notation as above, given a point x on M , for the preferred lift we are making choices between x' and $\tau(x')$. The choice could be made by requiring all $\Gamma_j > 0$ for example. However, that turns out not to be convenient for calculations, so we allow an arbitrary choice for each x_j .

Thus, given any point $(x'_1, \dots, x'_N) \in \widetilde{M}^N \setminus \widetilde{\Delta}$ the system on \widetilde{M} consists of $2N$ vortices at points $\{x'_1, \dots, x'_N, \tau(x'_1), \dots, \tau(x'_N)\}$. The scalar vorticity at x'_j is Γ_j and at $\tau(x'_j)$ is $-\Gamma_j$.

Using (2.3), the Hamiltonian is given by

$$\begin{aligned} \mathcal{H}_{\widetilde{M}}(x_1, \dots, x_N) = & - \sum_{i < j} \Gamma_i \Gamma_j \widetilde{G}(x'_i, x'_j) - \sum_{i < j} \Gamma_i \Gamma_j \widetilde{G}(\tau(x'_i), \tau(x'_j)) + \sum_{i \neq j} \Gamma_i \Gamma_j \widetilde{G}(x'_i, \tau(x'_j)) \\ & + \sum_j \Gamma_j^2 \widetilde{G}(x'_j, \tau(x'_j)) - \frac{1}{2} \sum_j \Gamma_j^2 \widetilde{R}(x'_j) - \frac{1}{2} \sum_j \Gamma_j^2 \widetilde{R}(\tau(x'_j)) \end{aligned} \quad (2.4)$$

where $\widetilde{G}(x, y)$ is the hydrodynamic Green's function and \widetilde{R} the Robin function on \widetilde{M} .

However, an adjustment needs to be made to (2.4): for justification, we return to the body of fluid on \widetilde{M} . Due to the absence of external forces, the total energy of the fluid is given by the surface integral $\int_{\widetilde{M}} \frac{1}{2} \rho |v|^2 ds$, where ρ is the constant density of the fluid and v its velocity. Transferring to the flow on M means that we only consider half of the fluid; therefore, the total energy must be divided by 2. With this, we conclude that the total energy of the fluid on M will be given by

$$\begin{aligned} \mathcal{H}(x_1, \dots, x_N) = & - \frac{1}{2} \sum_{i < j} \Gamma_i \Gamma_j \widetilde{G}(x'_i, x'_j) - \frac{1}{2} \sum_{i < j} \Gamma_i \Gamma_j \widetilde{G}(\tau(x'_i), \tau(x'_j)) + \frac{1}{2} \sum_{i \neq j} \Gamma_i \Gamma_j \widetilde{G}(x'_i, \tau(x'_j)) \\ & + \frac{1}{2} \sum_j \Gamma_j^2 \widetilde{G}(x'_j, \tau(x'_j)) - \frac{1}{4} \sum_j \Gamma_j^2 \widetilde{R}(x'_j) - \frac{1}{4} \sum_j \Gamma_j^2 \widetilde{R}(\tau(x'_j)) \end{aligned} \quad (2.5)$$

Since τ is a globally defined isometry of \widetilde{M} it follows that both \widetilde{G} and \widetilde{R} are invariant under τ , which implies some of these terms coincide.

Suppose that we fix y' , a preferred lift of y and x' , a preferred lift of x . Observe how (2.5) is unaffected by which of the two preimages we choose to be our preferred lift, so we are free to pick either one. This allows us to express functions on M through ones on \widetilde{M} :

Definition 2.3. *We define the twisted Green's function on M as*

$$G_M(x, y) = \widetilde{G}(x', y') - \widetilde{G}(x', \tau(y')) \quad (2.6)$$

and the (regular) Robin function on M as

$$R_M(x) = \tilde{R}(x') - \tilde{G}(x', \tau(x')) \quad (2.7)$$

Proposition 2.4. G_M is indeed a twisted Green's function of the Laplacian on M , and $R_M(x)$ is the Robin function of $G_M(x, y)$.

Proof. Consider the Laplacian of G_M as a function on \widetilde{M} :

$$\Delta_{x'} \left(\tilde{G}(x', y') - \tilde{G}(x', \tau(y')) \right) = \delta_{y'}(x') - \delta_{\tau(y')}(x')$$

For a fixed y (and, consequently, y') $\Delta_{x'} \left(\tilde{G}(x', y') - \tilde{G}(x', \tau(y')) \right)$ descends to M as a twisted function $\tilde{\delta}_y(x)$. Analogously to the regular Dirac delta function, it indicates when one of the preimages of x on \widetilde{M} coincides with one of the preimages of y on \widetilde{M} .

As one can easily see, G_M depends on the choice of the preferred lift, since it is twisted in both of its variables.

Now we want to check that R_M coincides with the desingularization of G_M .

Saying that $x \rightarrow y$ for two points $x, y \in M$ is equivalent to one of the two statements for \widetilde{M} : $x' \rightarrow y'$ or $x' \rightarrow \tau(y')$. Observe, however, that R_M , despite being a limit, is a function of one variable only and is therefore covered by a function on \widetilde{M} .

Thus, we are restricted to one lift only: either $x' \rightarrow y'$ or $x' \rightarrow \tau(y')$, depending on τ and our choice of preferred lifts. Since x' is a 'mute' variable, it does not matter which of the two options we choose, as it can be seen from the calculations below.

We have from (1.3) and (2.7):

$$\begin{aligned} \tilde{R}(y') - \tilde{G}(y', \tau(y')) &= \lim_{x' \rightarrow y'} \left(\tilde{G}(y', x') - \frac{1}{2\pi} \log d(y', x') - \frac{1}{2} \tilde{G}(y', \tau(x')) - \frac{1}{2} \tilde{G}(x', \tau(y')) \right) \\ &= \lim_{x' \rightarrow y'} \left(\frac{1}{2} \tilde{G}(y', x') + \frac{1}{2} \tilde{G}(\tau(y'), \tau(x')) - \frac{1}{2\pi} \log d(y', x') - \right. \\ &\quad \left. - \frac{1}{2} \tilde{G}(y', \tau(x')) - \frac{1}{2} \tilde{G}(x', \tau(y')) \right) \\ &= \lim_{x' \rightarrow y'} \left(G_M(y', x') - \frac{1}{2\pi} \log d(y', x') \right). \end{aligned} \quad (2.8)$$

Since we choose one lift out of two, explicit form of $\tilde{R}(\tau(y')) - \tilde{G}(y', \tau(y'))$ is the limit with $\tau(x') \rightarrow \tau(y')$, which can be shown to coincide with (2.8). Hence, $R_M(x)$ is a regular function on M , independent of our choice of the preferred lift. \square

This enables us to rewrite (2.4) as

$$\mathcal{H}(x_1, \dots, x_N) = - \sum_{i < j} \Gamma_i \Gamma_j G_M(x_i, x_j) - \frac{1}{2} \sum_j \Gamma_j^2 R_M(x_j) \quad (2.9)$$

Since exchanging x' with $\tau(x')$ also involves changing the sign of the corresponding Γ , it is clear from (2.4) that this Hamiltonian function \mathcal{H} is well-defined on $M \times \dots \times M \setminus \Delta$.

Notice that even if the Robin function on \widetilde{M} is constant, the one on M may not be, because of the term $\widetilde{G}(x', \tau(x'))$. For example, on the projective plane with the usual metric the Robin function is constant, while on the Möbius band and Klein bottle it is not.

To finish formalizing the Hamiltonian approach, we establish the symplectic form on the phase space:

Lemma 2.5. *The symplectic form on $\widetilde{M} \times \dots \times \widetilde{M} \setminus \widetilde{\Delta}$ from Proposition 2.2 is given by $\bigoplus_{k=1}^N \Gamma_k \sigma_k$, where σ_j is the symplectic form on j th copy of \widetilde{M} .*

Proof. The vorticity of the fluid on the j th copy of \widetilde{M} is given by $\Gamma_j \delta_{x'_j} \sigma - \Gamma_j \delta_{\tau(x'_j)} \sigma$. Due to the symmetries of our system, if the velocity of the point x'_j is given by a vector v , the velocity of $\tau(x'_j)$ will be $d\tau(v)$. Hence, the calculation of the symplectic form as in [20] gives us

$$\Omega_\lambda(\mathbf{u}, \mathbf{v}) = \sum_j \Gamma_j \sigma_{x'_j}(u_j, v_j) - \Gamma_j \sigma_{\tau(x'_j)}(d\tau(u_j), d\tau(v_j)) = 2 \sum_j \Gamma_j \sigma_{x'_j}(u_j, v_j),$$

since $\tau^* \sigma = -\sigma$. We have divided the Hamiltonian by 2 and therefore have to do the same to the symplectic form, obtaining the statement of the lemma. Note that this symplectic form is independent of our choice of preferred lift. \square

Remark 2.6. By the symmetric placement of vortices on \widetilde{M} , the stream function $\psi_{\widetilde{M}}$ on \widetilde{M} is

$$\psi_{\widetilde{M}}(x) = \sum_k \Gamma_k \left(\widetilde{G}(x, x_k) - \widetilde{G}(x, \tau(x_k)) \right),$$

where x_k and $\tau(x_k)$ are the centres of the point vortices and their copies respectively.

Observe that $\psi_{\widetilde{M}}$ is a twisted function in x : $\psi_{\widetilde{M}}(\tau(x)) = -\psi_{\widetilde{M}}(x)$. However, $\psi_{\widetilde{M}}$ is not sensitive to exchanging x_k and $\tau(x_k)$, since that changes not only the sign of $G(x, x_k) - G(x, \tau(x_k))$, but the sign of Γ_k as well.

This makes sense from the hydrodynamic point of view: the descent of $\psi_{\widetilde{M}}$ to M , the stream function ψ_M , must be a twisted function of $x \in M$ ([31]), unaffected by our choice of preferred lift.

Remark 2.7. For a single vortex on M (corresponding to two on \widetilde{M}) the Laplacian of the stream function will be

$$\Delta \psi_{\widetilde{M}} = \Gamma(\delta_{y'}(x') - \delta_{\tau(y')}(x')), \quad (2.10)$$

which we write as a function on \widetilde{M} and which, as we already know, descends to a twisted function on M . However, bear in mind (2.10) was written on \widetilde{M} interpreting Γ as a scalar; an assumption that cannot be made for M . Therefore, when writing vorticity-as-a-scalar intrinsically on M , we 'delegate' the twistedness to Γ , as we did at the end of Section 2.2.

This is done in the following way: for a fixed $y \in M$, we lift the regular delta function $\delta_y x$ to \widetilde{M} , to obtain $\delta'_y x' + \delta_{\tau(y')} x'$. However, by placing point vortices of strengths Γ and $-\Gamma$ at y' and $\tau(y')$ respectively, we 'twist' it, making it into (2.10).

2.5 The momentum map

Suppose a (connected) Lie group G acts by isometries on M and denote its Lie algebra by \mathfrak{g} . We describe the (possibly local) momentum map on the phase space associated to this action.

The action lifts to an orientation-preserving action of G by isometries on \widetilde{M} ([11]); therefore, the action in question is symplectic.

Consider an element $\xi \in \mathfrak{g}$ and let $\xi_{\widetilde{M}}$ be the associated vector field of the infinitesimal action on \widetilde{M} . Then, since the action of G on \widetilde{M} is the lift of one on M , $d\tau(\xi(x)) = \xi(\tau(x))$, i.e. $\xi_{\widetilde{M}}$ is a regular vector field.

Let $\psi : \widetilde{M} \rightarrow \mathfrak{g}^*$ be the associated momentum map (which exists globally provided the cohomological obstruction vanishes—if it does not vanish then the map exists locally). The map ψ is defined up to a constant by the equation

$$\langle d\psi_x(v), \xi \rangle = \sigma_x(\xi_{\widetilde{M}}(x), v), \quad (2.11)$$

where v is any vector field on \widetilde{M} .

Now take v such that it descends to M as a regular vector field and consider the application of τ to both sides of (2.11):

$$\langle d\psi_{\tau(x)}(d\tau(v)), \xi \rangle = ((\tau^{-1})^*\sigma)_{\tau(x)}(d\tau(\xi_{\widetilde{M}}(x)), d\tau(v)) = -\sigma_x(\xi_{\widetilde{M}}(x), v).$$

Therefore, $d\psi(x) = -d\psi(\tau(x))$, and $\psi : \widetilde{M} \rightarrow \mathfrak{g}^*$ is a twisted function.

On the phase space, the momentum map $\Phi : \widetilde{M}^N \rightarrow \mathfrak{g}^*$ is the usual one given by

$$\Phi(z_1, \dots, z_N) = \sum_j \Gamma_j \psi(z_j).$$

Applying τ to any of the z_j reverses both ψ and Γ_j and thereby leaves this expression unchanged. This momentum map therefore descends to a map (rather than a twisted map) $M \times \dots \times M \rightarrow \mathfrak{g}^*$.

3 Vortex motion on a Möbius band

In this section we apply all the apparatus developed above to the setting of vortex motion on the Möbius band. We adopt the boundary-free model of the Möbius band as a strip of fixed width πr and infinite height in the plane with opposite sides identified with opposite orientation: this infinite model of the Möbius band has no boundary, so we do not need to consider vortex-boundary interactions. If we denote the coordinate on the strip as $z = x + iy$, its real part has to be considered modulo πr .

The double cover of this model is a cylinder $\mathbb{C}/2\pi r\mathbb{Z}$ of circumference $2\pi r$ and coordinates (x, y) . We orient this by $dx \wedge dy$. The imaginary line that we draw on the cylinder to signify the division we will further refer to as *the imaginary boundary*. Figure 1 depicts our model; the blue arrows in it and all following figures indicate the oppositely oriented sides of the imaginary boundary, and the dashed horizontal line is the line $y = 0$. As a quotient of the cylinder, the Möbius band is obtained by identifying (x, y) with $\tau(x, y)$, where τ is the orientation reversing isometry given by $\tau(x, y) = (x + \pi r, -y)$.

The cylinder has symmetry group $O(2) \times E(1)$, where $E(1)$ is the Euclidean group for the line. The subgroup consisting of those elements commuting with τ descends to symmetries of the Möbius band. This subgroup is $O(2) \times \mathbb{Z}_2$, where \mathbb{Z}_2 acts by $(x, y) \mapsto (x, -y)$.

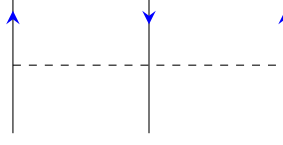


Figure 1: Two copies of the model of the Möbius band, covered by a cylinder. We refer to the vertical lines as the ‘imaginary boundary’. The dashed line is where $y = 0$.

3.1 Equations of motion

For brevity, we will refer to the pair (z, Γ) , i.e., the complex planar coordinate of the vortex centre and the vortex strength, as *vortex parameters*, or just *parameters*.

The dynamics of a vortex with parameters (z, Γ) will be covered by the dynamics of two vortices on the cylinder: one with parameters (z, Γ) and the other $(\bar{z} + \pi r, -\Gamma)$.

The Hamiltonian for the cylinder reads (see [22]):

$$\mathcal{H} = -\frac{1}{2\pi} \sum_{k < l} \Gamma_k \Gamma_l \log \left| \sin \frac{z_k - z_l}{2r} \right|,$$

or, as expressed through x - y coordinates,

$$\mathcal{H} = -\frac{1}{4\pi} \sum_{k < l} \Gamma_k \Gamma_l \log \left[\sin^2 \left(\frac{x_k - x_l}{2r} \right) + \sinh^2 \left(\frac{y_k - y_l}{2r} \right) \right].$$

We periodize the Hamiltonian as in Section 2.4 to obtain the explicit formula for the Möbius band Hamiltonian:

$$\begin{aligned} \mathcal{H} = & -\frac{1}{4\pi} \sum_{k < l} \Gamma_k \Gamma_l \log \left(\sin^2 \left(\frac{x_k - x_l}{2r} \right) + \sinh^2 \left(\frac{y_k - y_l}{2r} \right) \right) + \\ & + \frac{1}{4\pi} \sum_{k < l} \Gamma_k \Gamma_l \log \left(\cos^2 \left(\frac{x_k - x_l}{2r} \right) + \sinh^2 \left(\frac{y_k + y_l}{2r} \right) \right) + \\ & + \frac{1}{8\pi} \sum_k \Gamma_k^2 \log \left(1 + \sinh^2 \left(\frac{y_k}{r} \right) \right); \end{aligned} \quad (3.1)$$

The last term is the Robin function R_M . We can easily see how it is unaffected by the change of the local orientation or the exchange of the covering vortices.

Writing the system of equations on one chart, we obtain:

$$\begin{cases} \dot{x}_k = -\frac{1}{8\pi r} \sum_{l \neq k} \Gamma_l \frac{\sinh\left(\frac{y_k - y_l}{r}\right)}{\sin^2\left(\frac{x_k - x_l}{2r}\right) + \sinh^2\left(\frac{y_k - y_l}{2r}\right)} + \frac{1}{8\pi r} \sum_{l \neq k} \Gamma_l \frac{\sinh\left(\frac{y_k + y_l}{r}\right)}{\cos^2\left(\frac{x_k - x_l}{2r}\right) + \sinh^2\left(\frac{y_k + y_l}{2r}\right)} \\ \quad + \frac{1}{4\pi r} \Gamma_k \tanh\left(\frac{y_k}{r}\right), \\ \dot{y}_k = \frac{1}{8\pi r} \sum_{l \neq k} \Gamma_l \frac{\sin\left(\frac{x_k - x_l}{r}\right)}{\sin^2\left(\frac{x_k - x_l}{2r}\right) + \sinh^2\left(\frac{y_k - y_l}{2r}\right)} + \frac{1}{8\pi r} \sum_{l \neq k} \Gamma_l \frac{\sin\left(\frac{x_k - x_l}{r}\right)}{\cos^2\left(\frac{x_k - x_l}{2r}\right) + \sinh^2\left(\frac{y_k + y_l}{2r}\right)}. \end{cases} \quad (3.2)$$

Remark 3.1. One can see that changing the value of r can be compensated by rescaling x, y and time, so from now on we assume that $r = 1$.

In the framework of this model, a point vortex moves as it would on an oriented manifold, as long as it does not cross the imaginary boundary. If that happens, the vortex has to 'jump' to the other side of the strip, change the sign of its y coordinate and the sign of its strength.

This setup might seem unnatural, but the intuitive approach to vortex motion had to be sacrificed in order to have local orientation and be able to treat Γ s as scalars. However, this perception does not lead to a contradiction: crossing the imaginary boundary is the same as changing orientation of a small area surrounding the vortex, and therefore Γ has to change its sign.

3.2 Invariants and relative equilibria

Definition 3.2. *The transformation that takes all the vortices (Γ_i, z_i) on the cylinder covering the given one on the Möbius band into the system $(-\Gamma_i, \bar{z}_i - \pi)$ we call the Möbius flip.*

This is the formalization of the 'vortex jump'; however, in this case the vortex need not be on the imaginary boundary.

The Möbius flip on the cylinder is the involution τ from Sec. 2.1; therefore, applying it to all the point vortices must leave the Hamiltonian and the equations unchanged (this is easy to check with the explicit form of the Hamiltonian (3.1)). Additionally, it is easy to check that the local Hamiltonian equations are not affected by the change of orientation.

Observe that invariance under the Möbius flip implies that the location of the imaginary boundary does not affect our motion; this illustrates that the equations are well-defined.

As described above, the system on the Möbius band has a one-parameter group of Hamiltonian symmetries inherited from the cylinder: $SO(2)$ acting by horizontal translations, giving rise to a conserved quantity $\Phi := \sum_i \Gamma_i y_i$. As in the discussion in Section 2.5, Φ is a regular function: indeed, changing the orientation changes the signs of y_j together with Γ_j , and the function stays unchanged.

It is immediate from the form of the symmetry group that relative equilibria are horizontally moving rigid configurations of point vortices.

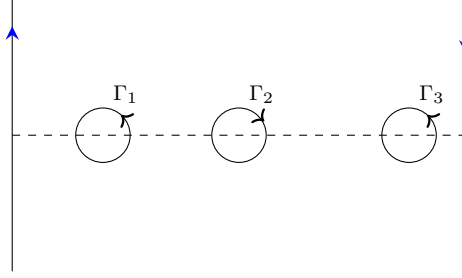
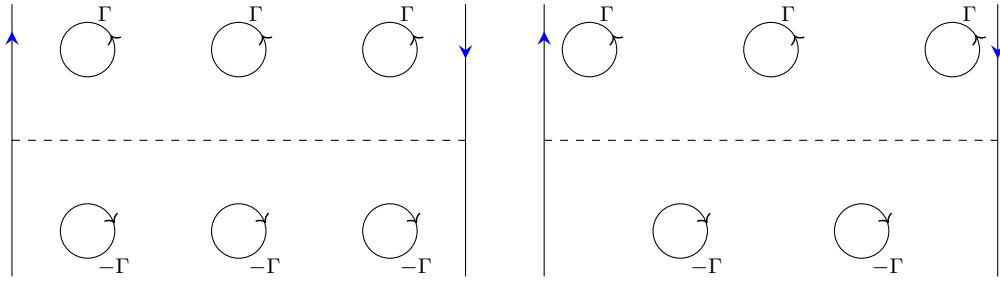
3.3 A general class of equilibria

It was pointed out in [22] that on the cylinder, given a sequence of $2N$ point vortices placed around a horizontal circle, with vorticities of alternating signs, then for the given cyclic ordering there is an equilibrium point (it is not known whether or not this is unique, although numerical experiment suggests it is for $N = 3$).

For such a configuration to arise from one on the Möbius band, the set of points must be τ -invariant, and moreover $\Gamma_x = -\Gamma_{\tau x}$. For this to be compatible with having alternating signs of vorticity, N must be odd.

Proposition 3.3. *In a preferred chart, consider the set of all configurations $\{(x_j, 0) \mid j = 1, \dots, N\}$ with $0 \leq x_1 < x_2 < \dots < x_N \leq \pi$, and with vorticities of alternating signs: $\Gamma_j \Gamma_{j+1} < 0$ for $j = 1, \dots, N-1$ and where N is odd. Then there is an equilibrium configuration in this set (see Figure 2).*

Proof. Consider the domain of these configurations. The Hamiltonian is a function of the x_j which tends to $+\infty$ as the configuration tends to the boundary (i.e. two vortices tend to a collision). It follows that in the interior of the domain, the Hamiltonian must attain a maximum. This critical point will be an equilibrium of the system. \square

Figure 2: A typical equilibrium configuration for $N = 3$ (a) A vertically aligned N -ring RE for even values of N (here $N = 6$).(b) A vertically staggered N -ring RE for odd values of N (here $N = 5$).Figure 3: The two types of N -ring relative equilibrium on a Möbius band

A particular instance of this is where, in our preferred chart, the points have alternating vorticity $\Gamma, -\Gamma, \dots$ and placed at the vertices of a regular N -gon (for odd N).

3.4 The N -ring relative equilibria

These configurations are more easily described on the cylinder. Consider a regular ring of $N \geq 1$ identical vortices with vorticity $\Gamma \neq 0$ on a horizontal circle with common vertical coordinate $y > 0$. Together with this consider the ‘antipodal ring’, the image of the first ring under the involution τ , and with vorticities $-\Gamma$. It has common vertical coordinate $-y$.

Note that if N is even, then the two rings are vertically aligned, while if N is odd they are vertically staggered. In terms of $O(3)$ and the Schönflies notation, for even N the configuration has symmetry D_{Nh} while for odd N it has symmetry D_{Nd} (see for example [18, Table 2] for this notation).

Since these configurations are invariant under τ they project to single rings with N vortices on the Möbius band. We call these N -rings; they are illustrated in Figure 3. If $N = 1$ this is the single point vortex described in Section 3.5 below.

Theorem 3.4. *On the Möbius band, an N -ring is a relative equilibrium.*

Suppose that the N -ring in question is an aligned one: that means N is an even number. Then if the strength of the vortices in the upper row is Γ and their vertical coordinate y , the

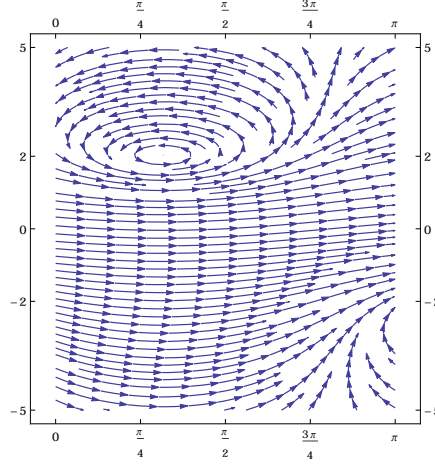


Figure 4: Instantaneous fluid flow induced by a solitary vortex on the Möbius band.

angular velocity is given by

$$\xi_a = \begin{cases} \frac{\Gamma N}{4\pi} \coth\left(\frac{Ny}{2}\right) & \text{if } N/2 \text{ is even} \\ \frac{\Gamma N}{4\pi} \coth(Ny) & \text{if } N/2 \text{ is odd.} \end{cases} \quad (3.3)$$

On the other hand, the angular velocity of staggered equilibria (N odd) is given by

$$\xi_s = \frac{\Gamma}{8\pi} (\tanh(y) - \coth(y)) + \frac{\Gamma N}{4\pi} \coth(2Ny). \quad (3.4)$$

A simple symmetry argument using the symmetries D_{Nh} and D_{Nd} mentioned above, demonstrates that such configurations are, indeed, relative equilibria. The momentum value at the ring is $N\Gamma y$, so those at different heights arise for different values of the momentum. For detailed calculations of the velocities, see Appendix A.

On the universal cover (the plane) these N -rings lift to von Kármán vortex streets, see for example [13].

3.5 Motion of a single vortex

A well-known fact is that a single vortex on a cylinder, sphere or plane remains stationary. As we see below, this is not the case in general for the Möbius band, and the equation of motion of one vortex is derived from (3.2) and is due solely to the Robin function in (3.1):

$$\begin{cases} \dot{x} = \frac{1}{4\pi} \Gamma \tanh y, \\ \dot{y} = 0; \end{cases}$$

showing that a vortex is stationary if and only if it lies on the line $y = 0$.

From the system of equations (3.2) we obtain the streamlines of one vortex on the band: see Figure 4. As time progresses, the vector field translates horizontally with the vortex.

For this case, let us demonstrate the construction of a global vector field (\dot{x}, \dot{y}) and investigate how the trajectories of motion come together. Due to non-orientability, the least number of covering charts for the Möbius strip is 2, which we will denote U_1 and U_2 .

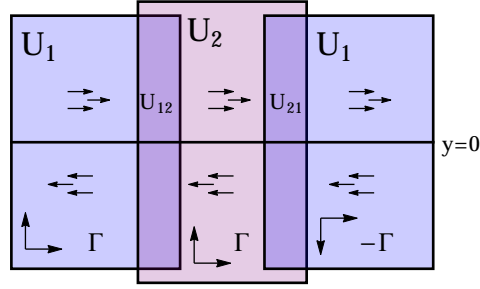


Figure 5: Two charts cover of a Möbius band. Horizontal arrows denote the direction of the horizontal vector field that is the solution of the Hamiltonian equations on each chart.

Let U_{12} be the left intersection of the charts, and U_{21} the right one as illustrated in Figure 5. The Jacobian of the coordinate change will be positive on U_{12} and negative on U_{21} .

We suppose that the vortex is initially placed on U_1 ; moving horizontally, it reaches U_{12} : the sign of its strength in local coordinates will not change transferring to U_2 . Once it reaches U_{21} , however, its strength will change its sign, and so will its y -coordinate. The resulting vector field is depicted in Figure 5.

Observe that despite each of the vector fields on the charts in Figure 5 being the solution of the Hamiltonian system of equations (as written on each of them) the resulting solution is **not** a vector field on the Möbius band. However, it is (and that is how we will interpret it) a distribution of the instantaneous velocities for given initial conditions of the system.

Despite this, the trajectories of motion are globally defined: due to changes in signs they can be glued together as the vortex moves from one chart to another.

4 Motion of two vortices

The equations of motion for the system with two point vortices are:

$$\begin{cases} \dot{x}_1 = -\frac{1}{8\pi} \left(\Gamma_2 \frac{\sinh(y_1 - y_2)}{\sin^2\left(\frac{x_1 - x_2}{2}\right) + \sinh^2\left(\frac{y_1 - y_2}{2}\right)} - \Gamma_2 \frac{\sinh(y_1 + y_2)}{\cos^2\left(\frac{x_1 - x_2}{2}\right) + \sinh^2\left(\frac{y_1 + y_2}{2}\right)} - 2\Gamma_1 \tanh(y_1) \right) \\ \dot{x}_2 = -\frac{1}{8\pi} \left(\Gamma_1 \frac{\sinh(y_2 - y_1)}{\sin^2\left(\frac{x_2 - x_1}{2}\right) + \sinh^2\left(\frac{y_2 - y_1}{2}\right)} - \Gamma_1 \frac{\sinh(y_2 + y_1)}{\cos^2\left(\frac{x_2 - x_1}{2}\right) + \sinh^2\left(\frac{y_2 + y_1}{2}\right)} - 2\Gamma_2 \tanh(y_2) \right) \\ \dot{y}_1 = \frac{\Gamma_2 \sin(x_1 - x_2)}{8\pi} \left(\frac{1}{\sin^2\left(\frac{x_1 - x_2}{2}\right) + \sinh^2\left(\frac{y_1 - y_2}{2}\right)} + \frac{1}{\cos^2\left(\frac{x_1 - x_2}{2}\right) + \sinh^2\left(\frac{y_1 + y_2}{2}\right)} \right) \\ \dot{y}_2 = \frac{\Gamma_1 \sin(x_2 - x_1)}{8\pi} \left(\frac{1}{\sin^2\left(\frac{x_2 - x_1}{2}\right) + \sinh^2\left(\frac{y_2 - y_1}{2}\right)} + \frac{1}{\cos^2\left(\frac{x_2 - x_1}{2}\right) + \sinh^2\left(\frac{y_2 + y_1}{2}\right)} \right) \end{cases} \quad (4.1)$$

To get an intuition about the motion, below we consider some of the simplest examples.

Example 4.1. Consider first, a 2-ring (as in Section 3.4), depicted in Figure 6.

If the initial coordinates of the centres are $(x_0, \pm y_0)$, Equation (4.1), as well as Theorem 3.4, yield $\dot{y}_i = 0$, $\dot{x}_i = \frac{1}{2\pi} \coth(2y_0)$.

In the preferred chart, both vortices will move horizontally towards the imaginary boundary, reach it, 'jump' to the other side, exchanging places, and then continue to move in the

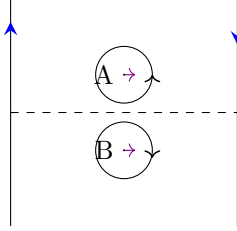


Figure 6: Two vortices with opposite vortex strength and centres arranged with vertical symmetry (a 2-ring in the terminology of Section 3.4) — see Example 4.1.

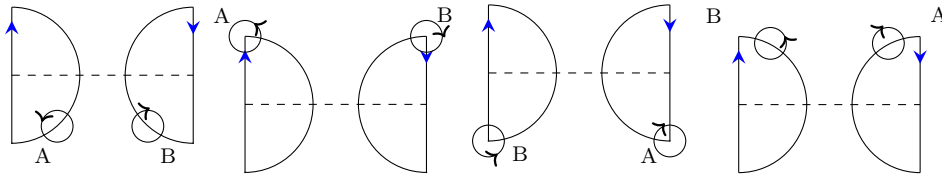


Figure 7: Schematic motion of two point vortices with horizontally symmetric placement of the centres; the semi-circles are approximate trajectories of their motion — see Example 4.2.

same fashion. Since the velocity of both vortex centres is the same, this configuration is an example of a relative equilibrium.

Example 4.2. In this case, let the two vortices again have opposite signs: $\Gamma_1 = -\Gamma_2$, but now be positioned symmetrically with respect to the line $x = \frac{\pi}{2}$. This configuration is fixed by the corresponding reflection in $O(2)$.

Denote the initial positions of the centres by (x_0, y_0) and $(\pi - x_0, y_0)$ respectively, and suppose that $y_0 < 0$ as illustrated in the leftmost part of Figure 7. Substituting these values into the equations (4.1) easily demonstrates that the symmetric arrangement of point vortex centres is preserved throughout the motion. The restriction of the Hamiltonian to this fixed point space is

$$\mathcal{H} = \frac{1}{4\pi} \log \left(\frac{\cos^2 x \cosh^2 y}{\sin^2 x + \sinh^2 y} \right).$$

Additionally, through drawing the level sets of the Hamiltonian, we can conclude that the motion goes as follows: two vortices start moving symmetrically in opposite directions towards the symmetry line; upon crossing the line $y = 0$ they start moving away from each other until they reach the imaginary boundary after the same finite amount of time, ‘jump over’ to the other side, go along the trajectory that the other used to occupy, reach the boundary and exchange places once more. This resembles a relative equilibrium on the plane, with two vortices going in a circle around their centre of vorticity, but here the trajectory is neither a circle, nor is such a configuration a relative equilibrium. Figure 7 illustrates four consecutive stages of motion.

Example 4.3. Here, we look at the asymptotic case: $y_1 = \infty$, with $\Gamma_1 > \Gamma_2 > 0$. Recalling the existence of the invariant $\Gamma_1 y_1 + \Gamma_2 y_2 = C$ and assuming that C is finite, we derive that $y_2 = -\infty$ and that $y_1 + y_2 = y_1 \left(1 - \frac{\Gamma_1}{\Gamma_2}\right) + \frac{C}{\Gamma_2} \rightarrow -\infty$. By taking limits of our system of

equations, we get

$$\begin{cases} \dot{x}_1 = -\frac{1}{4\pi}(2\Gamma_2 - \Gamma_1), \\ \dot{x}_2 = -\frac{1}{4\pi}\Gamma_2, \\ \dot{y}_1 = \dot{y}_2 = 0; \end{cases} \quad (4.2)$$

Due to the difference in velocities the motion will not be a relative equilibrium. Also, note that whether the two vortices are moving in the opposite or same directions depends on the relations between Γ_1 and Γ_2 .

4.1 Fixed equilibria

We continue by determining whether the general 2-vortex system has any fixed equilibrium points.

Fixed equilibria, as critical points of the Hamiltonian, correspond to zeros of (4.1). Observe that fixed equilibria have to have $x_1 - x_2 = 0$. This and a few manipulations turn (4.1) into

$$\begin{cases} 2\Gamma_2 \cosh y_1 \cosh y_2 = \Gamma_1 \sinh^2 y_1 - \Gamma_1 \sinh y_1 \sinh y_2, \\ 2\Gamma_1 \cosh y_1 \cosh y_2 = \Gamma_2 \sinh^2 y_2 - \Gamma_2 \sinh y_1 \sinh y_2. \end{cases} \quad (4.3)$$

Equating the right hand sides and solving as a quadratic equation for $\frac{\sinh y_2}{\sinh y_1}$ gives

$$\frac{\sinh y_2}{\sinh y_1} = 1 \text{ or } \frac{\sinh y_2}{\sinh y_1} = -\frac{\Gamma_1^2}{\Gamma_2^2}.$$

The first case is impossible, since our vortices would then occupy the same point. The second one enables us to rewrite the first equation in (4.1) as

$$2\sqrt{\Gamma_2^4 + \Gamma_1^4 \sinh^2 y_1} = \frac{\Gamma_1}{\Gamma_2} \frac{(\Gamma_1^2 + \Gamma_2^2) \sinh^2 y_1}{\sqrt{1 + \sinh^2 y_1}}, \quad (4.4)$$

which implies that fixed equilibria can only occur when Γ_1 and Γ_2 are of the same sign. Solving (4.1) yields

$$\begin{aligned} y_1 &= \pm \operatorname{arcsinh} \left(\sqrt{\frac{2\Gamma_2^2 \left(\Gamma_1^4 + \Gamma_2^4 + \sqrt{\Gamma_1^8 + \Gamma_1^6 \Gamma_2^2 + \Gamma_1^2 \Gamma_2^6 + \Gamma_2^8} \right)}{\Gamma_1^2 (\Gamma_1^2 - \Gamma_2^2)^2}} \right) \\ y_2 &= \mp \operatorname{arcsinh} \left(\sqrt{\frac{2\Gamma_1^2 \left(\Gamma_1^4 + \Gamma_2^4 + \sqrt{\Gamma_1^8 + \Gamma_1^6 \Gamma_2^2 + \Gamma_1^2 \Gamma_2^6 + \Gamma_2^8} \right)}{\Gamma_2^2 (\Gamma_1^2 - \Gamma_2^2)^2}} \right) \end{aligned} \quad (4.5)$$

The expression under the outer square roots is well-defined when $\Gamma_1 \neq \Gamma_2$. Thus, we have shown

Proposition 4.4. *When $\Gamma_1 \Gamma_2 > 0$ and $\Gamma_1 \neq \Gamma_2$, the system (4.1) is in a state of a fixed equilibrium when $x_1 = x_2$, and y_1, y_2 are as in (4.5).*

Notice from (4.5) that as $\Gamma_1 - \Gamma_2 \rightarrow 0$ so the equilibrium points tend to infinity.

For fixed distinct values of Γ_1 and Γ_2 of the same sign, we will call the two (opposite in sign) values of $\Phi(y_1, y_2) = \Gamma_1 y_1 + \Gamma_2 y_2$ at fixed equilibria the *equilibrium* values of the momentum map.

4.2 General motion of two vortices

In this section, we describe the motion of two point vortices in the more general case. To analyze our problem, we lift the two vortices of strengths Γ_1 and Γ_2 on the Möbius band to four on the cylinder, with strengths $\pm\Gamma_1, \pm\Gamma_2$, positioned with due symmetry.

Observation 4.5. Some key points ease our computations significantly:

- For a fixed orientation on the cylinder, the lift of the system on the Möbius band is unique;
- The symmetric arrangement of the vortices on the cylinder is preserved by the motion, therefore on the cylinder the trajectories of one pair of inequivalent vortices completely determines the motion of the whole system and the motion on the Möbius band as well. This way, we can observe only that inequivalent pair;
- Since it does not matter where we draw the imaginary boundary, we can safely assume the signs of Γ_i : we assume $\Gamma_1 > \Gamma_2 > 0$.
- The value of the globally defined momentum map on the cylinder is twice the value of the momentum map on the Möbius band; therefore, the y -coordinates of the two vortices that we choose to observe are related by $\Gamma_1 y_1 + \Gamma_2 y_2 = C$

The next step is to reduce the system. As stated above, we assume that $\Gamma_1 > 0, \Gamma_2 > 0$ and we have an invariant $\Gamma_1 y_1 + \Gamma_2 y_2 = C$. Expressing y_2 through y_1 , we substitute it into the system:

$$\begin{cases} \dot{x}_1 = -\frac{1}{8\pi} \left(\Gamma_2 \frac{\sinh\left(\frac{(\Gamma_2+\Gamma_1)y_1-C}{\Gamma_2}\right)}{\sin^2\left(\frac{x_1-x_2}{2}\right)+\sinh^2\left(\frac{(\Gamma_2+\Gamma_1)y_1-C}{2\Gamma_2}\right)} - \Gamma_2 \frac{\sinh\left(\frac{(\Gamma_2-\Gamma_1)y_1+C}{\Gamma_2}\right)}{\cos^2\left(\frac{x_1-x_2}{2}\right)+\sinh^2\left(\frac{(\Gamma_2-\Gamma_1)y_1+C}{2\Gamma_2}\right)} - 2\Gamma_1 \tanh(y_1) \right) \\ \dot{y}_1 = \frac{\Gamma_2 \sin(x_1-x_2)}{8\pi} \left(\frac{1}{\sin^2\left(\frac{x_1-x_2}{2}\right)+\sinh^2\left(\frac{(\Gamma_2+\Gamma_1)y_1-C}{2\Gamma_2}\right)} + \frac{1}{\cos^2\left(\frac{x_1-x_2}{2}\right)+\sinh^2\left(\frac{(\Gamma_2-\Gamma_1)y_1+C}{2\Gamma_2}\right)} \right) \\ \dot{x}_2 = -\frac{1}{8\pi} \left(-\Gamma_1 \frac{\sinh\left(\frac{(\Gamma_2+\Gamma_1)y_1-C}{\Gamma_2}\right)}{\sin^2\left(\frac{x_1-x_2}{2}\right)+\sinh^2\left(\frac{(\Gamma_2+\Gamma_1)y_1-C}{2\Gamma_2}\right)} - \Gamma_1 \frac{\sinh\left(\frac{(\Gamma_2-\Gamma_1)y_1+C}{\Gamma_2}\right)}{\cos^2\left(\frac{x_1-x_2}{2}\right)+\sinh^2\left(\frac{(\Gamma_2-\Gamma_1)y_1+C}{2\Gamma_2}\right)} - 2\Gamma_2 \tanh\left(\frac{C-\Gamma_1 y_1}{\Gamma_2}\right) \right) \\ \dot{y}_2 = -\frac{\Gamma_1}{\Gamma_2} \dot{y}_1 \end{cases} \quad (4.6)$$

We can reduce the system by one more degree of freedom: the right hand sides of all equations depend only on $x_1 - x_2$ and y_1 . We subtract the third equation from the first to get a system in two variables:

$$\begin{cases} \dot{x}_1 - \dot{x}_2 = -\frac{1}{8\pi} \left((\Gamma_2 + \Gamma_1) \frac{\sinh\left(\frac{(\Gamma_2+\Gamma_1)y_1-C}{\Gamma_2}\right)}{\sin^2\left(\frac{x_1-x_2}{2}\right)+\sinh^2\left(\frac{(\Gamma_2+\Gamma_1)y_1-C}{2\Gamma_2}\right)} - \right. \\ \quad \left. - (\Gamma_2 - \Gamma_1) \frac{\sinh\left(\frac{(\Gamma_2-\Gamma_1)y_1+C}{\Gamma_2}\right)}{\cos^2\left(\frac{x_1-x_2}{2}\right)+\sinh^2\left(\frac{(\Gamma_2-\Gamma_1)y_1+C}{2\Gamma_2}\right)} - 2\Gamma_1 \tanh(y_1) + 2\Gamma_2 \tanh\left(\frac{C-\Gamma_1 y_1}{\Gamma_2}\right) \right) \\ \dot{y}_1 = \frac{\Gamma_2 \sin(x_1-x_2)}{8\pi} \left(\frac{1}{\sin^2\left(\frac{x_1-x_2}{2}\right)+\sinh^2\left(\frac{(\Gamma_2+\Gamma_1)y_1-C}{2\Gamma_2}\right)} + \frac{1}{\cos^2\left(\frac{x_1-x_2}{2}\right)+\sinh^2\left(\frac{(\Gamma_2-\Gamma_1)y_1+C}{2\Gamma_2}\right)} \right) \end{cases} \quad (4.7)$$

The same reduction technique can be applied to the Hamiltonian, giving

$$\begin{aligned} \mathcal{H} = & -\frac{\Gamma_1 \Gamma_2}{4\pi} \log \left(\frac{\sin^2\left(\frac{x_1-x_2}{2}\right) + \sinh^2\left(\frac{y_1}{2} \left(1 + \frac{\Gamma_1}{\Gamma_2}\right) - \frac{C}{2\Gamma_2}\right)}{\cos^2\left(\frac{x_1-x_2}{2}\right) + \sinh^2\left(\frac{y_1}{2} \left(1 - \frac{\Gamma_1}{\Gamma_2}\right) + \frac{C}{2\Gamma_2}\right)} \right) + \\ & + \frac{\Gamma_1^2}{4\pi} \log(\cosh(y_1)) + \frac{\Gamma_2^2}{4\pi} \log\left(\cosh\left(\frac{C-\Gamma_1 y_1}{\Gamma_2}\right)\right) \end{aligned} \quad (4.8)$$

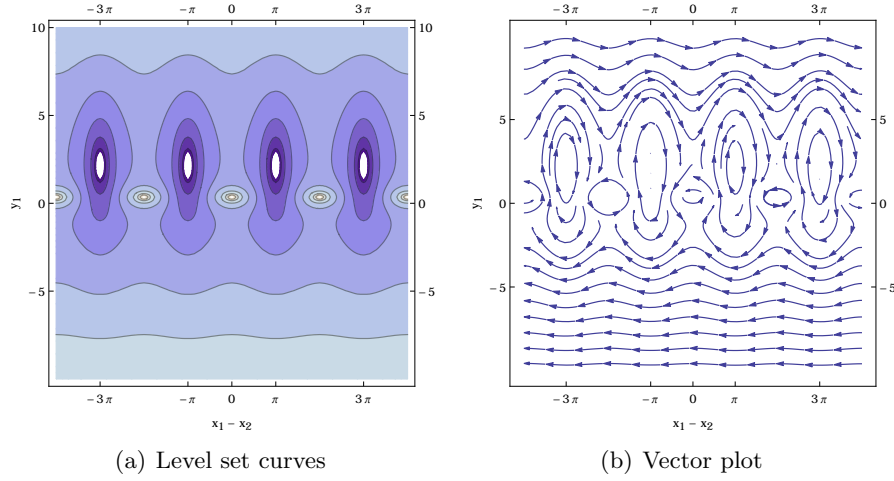


Figure 8: Level sets of the reduced Hamiltonian with the least number of critical points

Henceforth, our main goal is to reconstruct the motion of the initial system from the information we are able to obtain about the reduced one.

We start with searching for singular and critical points of the Hamiltonian. Without loss of generality, we may suppose that $-\pi \leq x_1 - x_2 \leq \pi$. However, in the pictures we draw four periods, to highlight the symmetries that the trajectories possess.

Noticing that the partial derivative $\frac{\partial \mathcal{H}}{\partial(x_1 - x_2)}$ is proportional to $\sin(x_1 - x_2)$ multiplied by some strictly negative function, we deduce that all the critical points lie on the lines $x_1 - x_2 = 0, \pm\pi$. Additionally, the Hamiltonian is 2π -periodic in $x_1 - x_2$ and symmetric with respect to the vertical axes listed above.

Assessing asymptotic behaviour of the function with a fixed $x_1 - x_2$ and $y_1 \rightarrow \pm\infty$ gives $\mathcal{H} \sim (\Gamma_1^2 - \Gamma_1\Gamma_2)|y|$. Therefore, $\mathcal{H} \rightarrow +\infty$ if $y_1 \rightarrow \pm\infty$.

- $x_1 - x_2 = 0$.

$$\begin{aligned} \mathcal{H} = & -\frac{\Gamma_1\Gamma_2}{2\pi} \log \left(\frac{\sinh^2 \left(\frac{y_1}{2} \left(1 + \frac{\Gamma_1}{\Gamma_2} \right) - \frac{C}{2\Gamma_2} \right)}{\cosh^2 \left(\frac{y_1}{2} \left(1 - \frac{\Gamma_1}{\Gamma_2} \right) + \frac{C}{2\Gamma_2} \right)} \right) + \\ & + \frac{\Gamma_1^2}{\pi} \log(\cosh(y_1)) + \frac{\Gamma_2^2}{\pi} \log \left(\cosh \left(\frac{C - \Gamma_1 y_1}{\Gamma_2} \right) \right) \end{aligned}$$

Obviously, $y_1 = \frac{C}{\Gamma_1 + \Gamma_2}$ is a singular point, as the point of collision of the vortices Γ_1 and Γ_2 ; here, $\mathcal{H} \rightarrow +\infty$.

As we have stated above, when $y_1 \rightarrow \pm\infty$, $\mathcal{H} \rightarrow +\infty$, which means that on the line $x_1 - x_2 = 0$ there must exist at least two more critical points, both saddles: maximum in $x_1 - x_2$, minimum in y .

Both of these points are relative equilibria when C is not an equilibrium value; for each of two equilibrium values of C one of them turns into a fixed equilibrium.

Through estimates on the first and second derivatives of $\dot{x}_1 - \dot{x}_2$ as a function of y_1 it can be shown that no more critical points exist on this line.

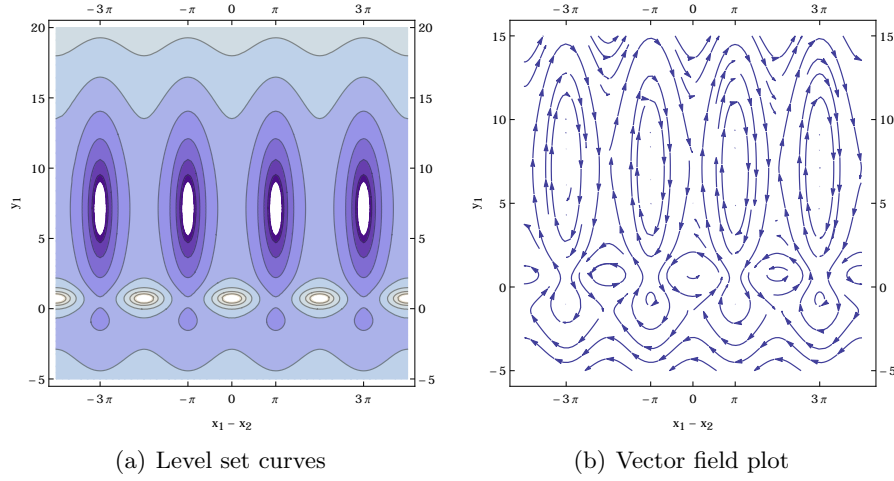


Figure 9: Level sets of the reduced Hamiltonian with two additional critical points

- $x_1 - x_2 = \pm\pi$

Here, the simplified Hamiltonian becomes

$$\mathcal{H} = -\frac{\Gamma_1\Gamma_2}{\pi} \log \left(\frac{\cosh^2 \left(\frac{y_1}{2} \left(1 + \frac{\Gamma_1}{\Gamma_2} \right) - \frac{C}{2\Gamma_2} \right)}{\sinh^2 \left(\frac{y_1}{2} \left(1 - \frac{\Gamma_1}{\Gamma_2} \right) + \frac{C}{2\Gamma_2} \right)} \right) + \\ + \frac{\Gamma_1^2}{\pi} \log (\cosh(y_1)) + \frac{\Gamma_2^2}{\pi} \log \left(\cosh \left(\frac{C - \Gamma_1 y_1}{\Gamma_2} \right) \right).$$

$y_1 = \frac{C}{\Gamma_1 - \Gamma_2}$ will always be a singular point, at which the Hamiltonian will be $-\infty$. Here, the collision happens between the vortices Γ_1 and $-\Gamma_2$.

Configurations as depicted in Figure 8 occur for certain values of the Γ_i and C ; however, another possibility exists, shown in Figure 9. In that case, the reduced Hamiltonian has an additional saddle point and a minimum below it. Observe that both are instances of relative equilibria that have the Γ_1 and $-\Gamma_2$ vortices on a vertical line above each other; however, as in Proposition 4.4 they cannot be fixed equilibria, as Γ_1 and Γ_2 have different signs on the chart on the Möbius band.

It seems (though the rigorous proof presents too big a computational challenge) that these are the two only possibilities. In principle, there could be any number of the saddle-minimum pairs on the lines $x_1 - x_2 = \pm\pi$, however this appears not to be the case.

For now we assume that $C \neq 0$ (we address the case of $C = 0$ separately below) and that the level sets of the Hamiltonian are similar to the ones in Figure 8, i.e. the Hamiltonian has no additional critical points on the lines $x_1 - x_2 = 0, \pm\pi$.

The trajectories as given by the level sets of the reduced Hamiltonian lack the information about the rotation around a cylinder. In what follows, we attempt to restore the motion of the system from the information provided to us in Figure 8.

Three types of curves are present in the picture: the closed trajectories going around the points with $(x_1 - x_2, y_1)$ coordinates $(2k\pi, \frac{C}{\Gamma_1 + \Gamma_2})$ (those we will refer to as Type I), closed

trajectories around the points of type $((2k+1)\pi, \frac{C}{\Gamma_1-\Gamma_2})$ (Type II) and the rest (Type III). The motion of the system will then be described by the

Theorem 4.6. *For two point vortices with Γ_1, Γ_2, C such that the Hamiltonian has the level sets as in Figure 8, we have the following:*

- *If the initial coordinates are in Regions I or II, the two vortices in consideration will rotate around each other, while simultaneously moving forward on the Möbius band as a pair. Due to continuous dependence of the integral, this motion will be periodic on a set of trajectories of planar measure 0.*
- *On trajectories of Type III, the vertical and the horizontal distances between the two vortices will change with a certain period, however, they will not rotate around each other. The two vortices may move in the same or opposite directions (both cases occur).*

Proof. In Regions I and II, the two vortices are rotating around each other; that is not the case for the Region III. In order to reconstruct the motion fully, however, we need some additional information, which we will be obtaining from certain limiting cases.

From the system (4.6) we observe that on every curve $\mathcal{C} = \{x_1 - x_2(t), y(t)\}$ \dot{x}_1 (as well as $\dot{x}_1 - \dot{x}_2$ and \dot{y}_1) is a function of $x_1 - x_2$ and y_1 . In order to restore the motion, we need to compute $\int_0^T \dot{x}_1 dt$, where T is the period of motion on the curve \mathcal{C} . We rewrite it tautologically as $\int_{\mathcal{C}} \frac{\dot{x}_1(x_1 - x_2, y_1)}{\sqrt{(\dot{x}_1 - \dot{x}_2)^2 + (\dot{y}_1)^2}} ds$, with ds the element of length on the curve \mathcal{C} . This quantity tells us how much the first vortex moves on the cylinder with every period of motion.

The motion of the system will be periodic in two cases: when the integral is 0, or, on a cylinder with circumference 2π , has the form $\frac{p}{q}\pi$, $p, q \in \mathbb{Z}$.

Firstly, we try to establish whether the integral in question is always equal to zero. For Region I, we suppose that our trajectory is very close to the point $(0, \frac{C}{\Gamma_1+\Gamma_2})$ (for Region II, it is the point $(\pm\pi, \frac{C}{\Gamma_1-\Gamma_2})$). On these trajectories, the pair of vortices that are very close together will mimic (to the rest of the system) the behaviour of one vortex with vorticity $\Gamma_1 + \Gamma_2$ ($\Gamma_1 - \Gamma_2$), see baby vortices section in [22].

In the case of four vortices this means that each pair of two closely placed vortices behaves like one bigger vortex. Therefore, the motion is very closely approximated by that of two vortices of opposite strengths on each side of the cylinder. This construction is stationary if and only if their vertical coordinates are zero, which is not the case, since $C \neq 0$. Therefore, the value of the integral is not identically equal to zero and the translational component is present in the motion of the system.

In order to proceed, we require a few lemmas:

Lemma 4.7. $\int_{\mathcal{C}} \frac{\dot{x}_1}{\sqrt{(\dot{x}_1 - \dot{x}_2)^2 + (\dot{y}_1)^2}} ds$ for all curve types I, II and III continuously depends on the curve, i.e. on its starting point.

Proof. This is quite straightforward, as we can take any bounded subregion D that contains no critical points of the function but fully contains curves that intersect it and consider two

close curves \mathcal{C} and \mathcal{C}' within it. Then

$$\left| \int_{\mathcal{C}} \frac{\dot{x}_1}{\sqrt{(\dot{x}_1 - \dot{x}_2)^2 + (\dot{y})^2}} ds - \int_{\mathcal{C}'} \frac{\dot{x}_1}{\sqrt{(\dot{x}_1 - \dot{x}_2)^2 + (\dot{y})^2}} ds \right| < \\ < \max \left| \frac{\dot{x}_1}{\sqrt{(\dot{x}_1 - \dot{x}_2)^2 + \dot{y}_1^2}} \right| \left(\int_{\mathcal{C}} ds - \int_{\mathcal{C}'} ds \right) \rightarrow 0,$$

since all the functions $\frac{\partial \mathcal{H}}{\partial(x_1 - x_2)}$, $\frac{\partial \mathcal{H}}{\partial y_1}$, \mathcal{H} , as well as tangent vectors to the curves are bounded due to the choice of D \square

Lemma 4.8. *In the general case, the integral depends non-trivially on the path we choose.*

Proof. First, we establish this for Region I (for II, the statement can be proven similarly).

Suppose the configuration is very close to the singular point inside Region I, i.e. the two vortices are very close to each other. Therefore, when calculating the speed of rotation around each other, we may disregard the influence of the opposite pair of vortices, and the time required for the vortices to go one full circle will be

$$T \sim \epsilon^2 (\sim \epsilon, \text{ in Region II}),$$

where ϵ is the distance between vortices. The horizontal velocity of the vortex pair will be approximately

$$\dot{x}_1 \sim \frac{\Gamma_2 + \Gamma_1}{2\pi} \tanh(y_1).$$

The rotational speed is dependent on ϵ , unlike \dot{x}_1 . Therefore, depending on the initial point of the trajectory, a very different number of full turns will "fit" into a pair going full circle around the cylinder. Thus, the integral depends non-trivially on the trajectory.

For Region III two different cases exist: when C is not an equilibrium value and when it is.

Suppose C is not an equilibrium value; therefore, the two saddle critical points on the line $x_1 - x_2 = 0$ are relative equilibria. Since the motion depends continuously on the initial parameters, $\dot{x}_1 \neq 0$ on the trajectories near separatrices (and, consequently, relative equilibrium points). However, as we approach relative equilibria, $T \rightarrow \infty$ and, therefore, $\int_0^T \dot{x}_1 dt \rightarrow \infty$.

When C is an equilibrium value, non-triviality stems from different values of the integrals at two asymptotic cases. Suppose $C > 0$ and the y -coordinate of the relative equilibrium is greater than 0 as well (the opposite case can be tackled in similar way). As we approach the separatrix containing the equilibrium point, $\int_0^T \dot{x}_{1(2)} dt \rightarrow 0$, since the motion smoothly depends on the initial conditions. On the other hand, take $y_1 \rightarrow +\infty$, $y_2 \rightarrow -\infty$ (as in Example 3). Since the velocities are given by (4.2) and integral of $\dot{x}_1 - \dot{x}_2$ over the period T must be 2π ,

$$T = \frac{8\pi^2}{\Gamma_1 - \Gamma_2}.$$

Thus, when $y_1 \rightarrow +\infty$, $y_2 \rightarrow -\infty$, $\int_0^T \dot{x}_1 dt \rightarrow -\frac{2\pi(2\Gamma_2 - \Gamma_1)}{\Gamma_1 - \Gamma_2}$ and $\int_0^T \dot{x}_2 dt \rightarrow -\frac{2\pi\Gamma_2}{\Gamma_1 - \Gamma_2}$, at least one of which is not equal to 0. \square

Thus, for Regions I and II the integral $\int_0^T \dot{x}_1 dt$ will almost never be a rational multiple of π , and the motion will consist of rotation around each other and translating around the cylinder.

In Region III, when $2\Gamma_2 \geq \Gamma_1$, the pair of infinitely removed vortices will rotate in the same direction (meaning that $\int_0^T \dot{x}_1 dt$ and $\int_0^T \dot{x}_2 dt$ over the period of motion will have the same signs). When $2\Gamma_2 < \Gamma_1$, the directions of rotation are opposite (with the opposite signs of the two integrals). From the non-trivial and smooth dependence on the trajectory we conclude that it is almost never a rational number multiplied by π either.

Therefore, two types of motion can exist: when the two integrals have the same sign, the particles are moving in the same direction, and a difference between the horizontal components in their velocities allows the first integral to differ by $\pm 2\pi$. The picture is very much the same when they are moving in the opposite directions.

However, there seems to be nothing that would prevent one of the integrals from turning zero and then switching the sign: in this case the motion will turn periodic, with one vortex rotating and the other going around the cylinder. This might allow for the transfers between the two types of motion in the region. \square

If additional critical points (Figure 9) appear on lines $x_1 - x_2 = \pm\pi$, the motion around them will be of the same type as for Regions I and II. Additional non-closed trajectories will result in motion of the same type as in trajectories in Region III; the required proof of non-trivial and smooth dependence on the trajectory can be repeated verbatim.

Two cases remain unaddressed: those of $C = 0$ and $\Gamma_1 = \Gamma_2$. We start with the first one.

4.2.1 Zero momentum

Putting $C = 0$ makes (4.8) a symmetric function of y_1 , as can be easily observed from Figure 10. Thus, for a curve $\{(x_1 - x_2)(t), y_1(t)\}$ with period T in Regions I and II we have $(x_1 - x_2)(t + \frac{T}{2}) = -(x_1 - x_2)(t)y_1(t + \frac{T}{2}) = -y_1(t)$, giving

$$\begin{aligned}
 \int_0^T \dot{x}_1((x_1 - x_2)(t), y_1(t)) dt &= \int_0^{\frac{T}{2}} \dot{x}_1((x_1 - x_2)(t), y_1(t)) dt + \int_{\frac{T}{2}}^T \dot{x}_1((x_1 - x_2)(t), y_1(t)) dt = \\
 &= \int_0^{\frac{T}{2}} \dot{x}_1((x_1 - x_2)(t), y_1(t)) dt + \int_0^{\frac{T}{2}} \dot{x}_1(-(x_1 - x_2)(t), -y_1(t)) dt = \\
 &= \int_0^{\frac{T}{2}} \dot{x}_1((x_1 - x_2)(t), y_1(t)) dt - \int_0^{\frac{T}{2}} \dot{x}_1((x_1 - x_2)(t), y_1(t)) dt = 0,
 \end{aligned}
 \tag{4.9}$$

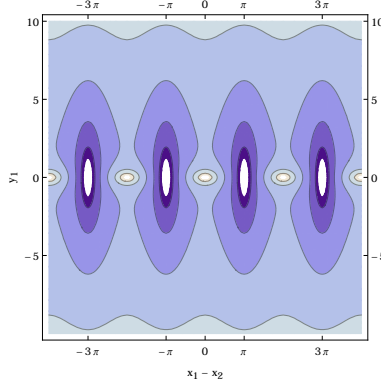


Figure 10: Level sets of the reduced Hamiltonian with zero value of momentum map

owing to the explicit form of \dot{x}_1 . Hence, the vortex pair does not rotate around the cylinder; the motion consists solely of the two vortices rotating around each other. However, for Region III the motion does not differ from the general case.

4.2.2 $\Gamma_1 = \Gamma_2$

When $\Gamma_1 = \Gamma_2$, the major difference occurring is that \mathcal{H} has a finite limit when $y \rightarrow \pm\infty$. As can be seen in Figure 11, the picture is symmetric, but now the symmetry is with respect to the line $y = \frac{C}{2}$, robbing us of the zero integral as in (4.9). Additionally, the critical point at $\frac{C}{\Gamma_1 - \Gamma_2}$ disappears, leaving us with trajectories of Types I and III only.

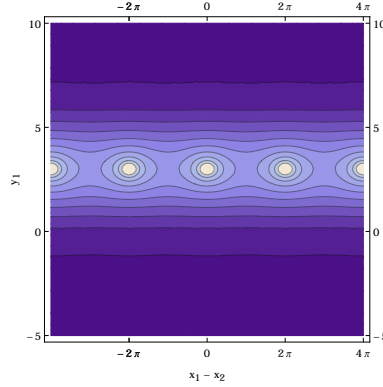
For Region I, we may employ precisely the same reasoning as we have before, for the non-zero C case. Region III, however, requires more caution.

If we set $\Gamma_1 = \Gamma_2$ in Example 3, the velocities of the two point vortices will coincide. This contradicts the fact that $\int_0^T \dot{x}_1 - \dot{x}_2 dt = \pm 2\pi$.

However, this paradox can be explained: as we have mentioned above, with $\Gamma_1 > \Gamma_2$ and $y_1 \rightarrow \pm\infty$, $\mathcal{H} \rightarrow \infty$ for all values of $x_1 - x_2$. This is not the case when $\Gamma_1 = \Gamma_2$: here the limit of \mathcal{H} with $y_1 \rightarrow \pm\infty$ will be equal to $\frac{1}{\cos^2\left(\frac{x_1 - x_2}{2}\right) + \cosh(C)}$. Therefore, the 'level set' of the Hamiltonian at $\pm\infty$ is not well-defined.

But we have another limiting case to draw the information from: when $x_1 - x_2 = \pm\pi$, we have precisely one relative equilibrium point: $y_1 = -y_2 = \frac{C}{2}$, where two vortices with opposite vorticity are above each other. As we have demonstrated in Example 2, they will move parallel to each other in the same direction. Therefore, on the trajectories very close to the separatrix we will have the two point vortices moving in the same direction.

Remark 4.9. When $\Gamma_1 = \Gamma_2$ and $C = 0$ (see Example 4.2), we do not have Region III; as can be checked, the Hamiltonian turns infinite in the lines $\frac{x_1 - x_2}{2} = \pm\pi$. This happens due to the fact that the separatrix from Region II stretches and goes to infinity as $\Gamma_2 \rightarrow \Gamma_1$ or vice versa. Thus, in those cases, all the motion is periodic and without additional rotation, as was demonstrated explicitly above.

Figure 11: Level sets of the reduced Hamiltonian for the case $\Gamma_1 = \Gamma_2$

5 Concluding remarks

A number of questions remain unanswered, the prime example being to prove that the maximal number of critical points of the Hamiltonian on the Möbius band is as depicted in Figure 9. Since this function has three independent parameters and complicated structure, all the standard approaches to a proof present considerable numerical difficulties.

The other problem is a description of fixed and relative equilibria for three point vortices. One can demonstrate that fixed equilibria on a straight vertical line must conform to the condition $\Gamma_1^2 y_1 + \Gamma_2^2 y_2 + \Gamma_3^2 y_3 = 0$, but the remaining conditions are hard to pin down.

A Velocity of the N-ring relative equilibria

Here we give a proof of the formulae for the angular velocities of the N -ring relative equilibria stated in Theorem 3.4.

We begin with the case of two aligned rings. As we have mentioned, $N = 2K$: therefore, K is the number of point vortices in the upper row on the chart on the Möbius band.

Without loss of generality we may assume that the leftmost vortex in the top row is positioned at $(0, y)$: the i th vortex in the top row is at $(\frac{\pi(i-1)}{K}, y)$, with similar coordinates for the lower row. Since the configuration is a relative equilibrium, we only need to determine the velocity of one of the vortices: we do it for the leftmost one in the upper row. After substituting the values above into (3.2), we get

$$\dot{x}_1 = \frac{\Gamma}{4\pi} (\tanh(y) + \coth(y)) + \frac{\Gamma}{8\pi} \sum_{j=1}^{K-1} \frac{\sinh(2y)}{\sin^2\left(\frac{\pi j}{K}\right) + \sinh^2(y)} + \frac{\sinh(2y)}{\cos^2\left(\frac{\pi j}{K}\right) + \sinh^2(y)} \quad (\text{A.1})$$

Lemma A.1. *The two sums above are given by*

$$\sum_{j=1}^K \frac{\sinh(2y)}{\sin^2\left(\frac{\pi j}{K}\right) + \sinh^2(y)} = 2K \coth(Ky)$$

and for the second,

$$\sum_{j=1}^K \frac{\sinh(2y)}{\cos^2\left(\frac{\pi j}{K}\right) + \sinh^2(y)} = \begin{cases} 2K \coth(Ky) & \text{if } K \text{ is even} \\ 2K \tanh(Ky) & \text{if } K \text{ is odd.} \end{cases}$$

Proof. We adapt the method posted on the stackexchange forum [14]: observe that the function

$$\frac{2K}{z(z^{2K} - 1)}$$

has residues 1 at $e^{\pi i j/K}$ (and $-2K$ at 0). For our first sum, consider the function

$$f(z) := \frac{2K}{z(z^{2K} - 1)} \frac{\sinh(2y)}{\sinh^2(y) + \left(\frac{z - \frac{1}{z}}{2i}\right)^2} = \frac{-8K}{(z^{2K} - 1)} \frac{\sinh(2y)z}{z^4 - 2z^2(1 + 2\sinh^2(y)) + 1} \quad (\text{A.2})$$

This rational function has poles at the $2K$ roots of unity, and at the four distinct points $\pm e^y, \pm e^{-y}$, which are the roots of

$$z^4 - 2z^2(1 + 2\sinh^2(y)) + 1 = (z^2 - e^{2y})(z^2 - e^{-2y})$$

(all the poles of f are simple).

To evaluate the sum, we note that the residue of f at $z = e^{i\pi j/K}$ is now

$$\frac{\sinh(2y)}{\sin^2(\pi j/K) + \sinh^2(y)}.$$

Since the sum of all the residues of f vanishes, to find the required sum we only need to calculate the remaining residues, and multiply their sum by $-1/2$ (since each term in the sum is counted twice). One finds,

$$\text{Res}(f, \pm e^y) = \frac{-2K}{e^{2Ky} - 1}, \quad \text{and} \quad \text{Res}(f, \pm e^{-y}) = \frac{2K}{e^{-2Ky} - 1}.$$

Summing these four residues and multiplying by $-\frac{1}{2}$ gives us the first sum of the lemma.

Analogously, we construct a rational function $g(z)$ for the second sum::

$$g(z) := \frac{2K}{z(z^{2N} - 1)} \frac{\sinh(2y)}{\sinh^2(y) + \left(\frac{z + \frac{1}{z}}{2}\right)^2} = \frac{8K}{(z^{2N} - 1)} \frac{z \sinh(2y)}{z^4 + 2z^2(1 + 2\sinh^2(y)) + 1}$$

In this case, we need to compute residues of $g(z)$ at poles located at $\pm ie^y$ and $\pm ie^{-y}$, the roots of $z^4 + 2z^2(1 + 2\sinh^2(y)) + 1$. We have,

$$\text{Res}(g, \pm ie^y) = \frac{-2K}{(-1)^K e^{2Ky} - 1}, \quad \text{and} \quad \text{Res}(g, \pm ie^{-y}) = \frac{2K}{(-1)^K e^{-2Ky} - 1}.$$

Summing these residues and multiplying by $-\frac{1}{2}$ gives us the second sum of the lemma. \square

Suppose K is even; using Lemma A.1, (A.1) becomes

$$\begin{aligned}\dot{x}_1 &= \frac{\Gamma}{2\pi} \coth(2y) + \frac{\Gamma}{8\pi} \left(4K \coth(Ky) - \frac{\sinh(2y)}{\sinh^2(y)} - \frac{\sinh(2y)}{\cosh^2(y)} \right) \\ &= \frac{\Gamma K}{2\pi} \coth(Ky),\end{aligned}\tag{A.3}$$

since in Lemma A.1 we have additionally counted $j = K$.

Using the same method for odd K , we get

$$\dot{x}_1 = \frac{\Gamma K}{2\pi} \coth(2Ky).$$

We act analogously when the two rows are staggered. However, in this case N is an odd number: we suppose that $N = 2K - 1$, and that the top row of vortices on the chart on the Möbius band has K vortices in it. Using the same notation, we observe that the horizontal distance between the leftmost vortex (which we assume to be above the line $y = 0$) and the other vortices in the upper row is $\frac{2\pi j}{2K-1}$, $j = 1, \dots, K-1$. In turn, horizontal distances between the same vortex and the vortices in the bottom row are given by $\frac{(2j-1)\pi}{2K-1}$, $j = 1, \dots, K-1$. Thus, we have for the velocity:

$$\dot{x}_1 = \frac{\Gamma}{4\pi} \tanh(y) + \frac{\Gamma \sinh(2y)}{8\pi} \sum_{j=1}^{K-1} \frac{1}{\sinh^2(y) + \sin^2\left(\frac{(2j-1)\pi}{2K-1}\right)} + \frac{1}{\sinh^2(y) + \cos^2\left(\frac{2j\pi}{2K-1}\right)}$$

We consider the expression $\sum_{j=1}^{K-1} \frac{1}{\sinh^2(y) + \sin^2\left(\frac{(2j-1)\pi}{2K-1}\right)} + \frac{1}{\sinh^2(y) + \cos^2\left(\frac{2j\pi}{2K-1}\right)}$ separately. One can observe that due to the fact that \sin and \cos are squared in the sum,

$$\begin{aligned}&\sum_{j=1}^{K-1} \left(\frac{1}{\sinh^2(y) + \sin^2\left(\frac{(2j-1)\pi}{2K-1}\right)} + \frac{1}{\sinh^2(y) + \cos^2\left(\frac{2j\pi}{2K-1}\right)} \right) \\ &= \frac{1}{2} \sum_{l=1}^{2K-2} \left(\frac{1}{\sinh^2(y) + \sin^2\left(\frac{l\pi}{2K-1}\right)} + \frac{1}{\sinh^2(y) + \cos^2\left(\frac{l\pi}{2K-1}\right)} \right),\end{aligned}$$

which reduces this sum to the one from Lemma A.1; in particular, the top limit of the sum is always an odd number. Therefore,

$$\begin{aligned}\dot{x}_1 &= \frac{\Gamma \tanh(y)}{4\pi} + \frac{\Gamma}{16\pi} \left((4K-2) \coth((2K-1)y) + (4K-2) \tanh((2K-1)y) \right. \\ &\quad \left. - \frac{\sinh(2y)}{\sinh^2(y)} - \frac{\sinh(2y)}{\cosh^2(y)} \right) \\ &= \frac{\Gamma}{8\pi} (\tanh(y) - \coth(y)) + \frac{\Gamma(2K-1)}{4\pi} \coth((4K-2)y).\end{aligned}\tag{A.4}$$

and recalling that $2K - 1 = N$, we get the statement of our theorem.

Remark A.2. It can be explicitly checked that (3.3) turns into $\frac{\Gamma}{2\pi} \coth(2y)$ when $N = 2$: this is Example 4.1. When $y \rightarrow 0$, $\xi_a \sim \frac{\Gamma}{4\pi y}$, consistent with the fact that the angular velocity tends to $+\infty$ when the two rows aligned are infinitely close.

When we substitute $N = 1$ in (3.4), we get the motion of one point vortex: and indeed, (3.4) readily becomes $\frac{\Gamma}{4\pi} \tanh(y)$. When $y = 0$, staggered N -rings become fixed equilibria. With $y \rightarrow 0$ the angular velocity ξ_s is given by

$$\xi_s = \frac{\Gamma y (1 + 2N^2)}{12\pi} + \bar{O}(y^3),$$

and becomes 0 when $y = 0$.

References

- [1] R. Abraham, J. E. Marsden, and T. Ratiu. *Manifolds, tensor analysis, and applications*, volume 75. Springer Science & Business Media, 2012.
- [2] H. Aref. Motion of three vortices. *The Physics of Fluids*, 22(3):393–400, 1979.
- [3] H. Aref. Point vortex dynamics: a classical mathematics playground. *Journal of mathematical Physics*, 48(6):065401, 2007.
- [4] H. Aref, J. B. Kadtke, I. Zawadzki, L. J. Campbell, and B. Eckhardt. Point vortex dynamics: recent results and open problems. *Fluid Dynamics Research*, 3(1-4):63, 1988.
- [5] H. Aref and M. A. Stremler. On the motion of three point vortices in a periodic strip. *Journal of Fluid Mechanics*, 314:1–25, 1996.
- [6] V. I. Arnold and B. A. Khesin. *Topological methods in hydrodynamics*, volume 125. Springer Science & Business Media, 1999.
- [7] N. A. Balabanova. A Hamiltonian approach for point vortices on non-orientable surfaces ii: the Klein bottle. *Preprint*, 2022.
- [8] S. Boatto and J. Koiller. Vortices on closed surfaces. In D. Chang, D. Holm, G. Patrick, and T. Ratiu, editors, *Geometry, Mechanics and Dynamics*, volume 73 of *Fields Institute Communications*. Springer, New York, NY., 2015.
- [9] A. Bossavit. Differential geometry for the student of numerical methods in electromagnetism. *Lecture notes. Available online on <http://butler.cc.tut.fi/~bossavit/Books/DGSNME/DGSNME.pdf>*, 1990.
- [10] R. Bott and L. W. Tu. *Differential forms in algebraic topology*, volume 82. Springer Science & Business Media, 2013.
- [11] G. E. Bredon. *Introduction to compact transformation groups*. Academic press, 1972.
- [12] D. G. Dritschel and S. Boatto. The motion of point vortices on closed surfaces. *Proceedings of the Royal Society A: Mathematical, Physical and Engineering Sciences*, 471(2176):20140890, 2015.
- [13] D. Hally. Stability of streets of vortices on surfaces of revolution with a reflection symmetry. *J. Math. Phys.*, 21:211–217, 1980.

-
- [14] <https://math.stackexchange.com/users/13854/robjohn>. Finite sum $\sum_{k=1}^{m-1} \frac{1}{\sin^2 \frac{k\pi}{m}}$. Mathematics Stack Exchange. URL:<https://math.stackexchange.com/q/2661896> (version: 2018-02-22).
 - [15] R. Kidambi and P. K. Newton. Motion of three point vortices on a sphere. *Physica D: Nonlinear Phenomena*, 116(1-2):143–175, 1998.
 - [16] G. Kirchhoff. Vorlesung uber mechanik, 1876.
 - [17] F. Laurent-Polz. Point vortices on the sphere: a case with opposite vorticities. *Nonlinearity*, 15(1):143, 2001.
 - [18] C. Lim, J. Montaldi, and M. Roberts. Point vortices on the sphere. *Physica D*, 148:97–135, 2001.
 - [19] C. Marchioro and M. Pulvirenti. *Mathematical theory of incompressible nonviscous fluids*, volume 96. Springer Science & Business Media, 2012.
 - [20] J. Marsden and A. Weinstein. Coadjoint orbits, vortices, and Clebsch variables for incompressible fluids. *Phys. D*, 7(1-3):305–323, 1983. Order in chaos (Los Alamos, N.M., 1982).
 - [21] J. Montaldi and C. Nava-Gaxiola. Point vortices on the hyperbolic plane. *J. Math. Phys.*, 55:102702, 1–14, 2014.
 - [22] J. Montaldi, A. Soulière, and T. Tokieda. Vortex dynamics on a cylinder. *SIAM Journal on Applied Dynamical Systems*, 2(3):417–430, 2003.
 - [23] P. K. Newton. *The N-vortex problem: analytical techniques*, volume 145. Springer Science & Business Media, 2013.
 - [24] K. A. O’Neil. On the hamiltonian dynamics of vortex lattices. *Journal of Mathematical Physics*, 30(6):1373–1379, 1989.
 - [25] S. Pekarsky and J. Marsden. Point vortices on a sphere: Stability of relative equilibria. *J. Math. Phys.*, 39(11):5894–5907, 1998.
 - [26] C. G. Ragazzo. The motion of a vortex on a closed surface of constant negative curvature. *Proceedings of the Royal Society A: Mathematical, Physical and Engineering Sciences*, 473(2206):20170447, 2017.
 - [27] C. G. Ragazzo and H. H. de Barros Viglioni. Hydrodynamic vortex on surfaces. *Journal of Nonlinear Science*, 27(5):1609–1640, 2017.
 - [28] T. Sakajo and Y. Shimizu. Point vortex interactions on a toroidal surface. *Proceedings of the Royal Society A: Mathematical, Physical and Engineering Sciences*, 472(2191):20160271, 2016.
 - [29] M. A. Stremler and H. Aref. Motion of three point vortices in a periodic parallelogram. *Journal of Fluid Mechanics*, 392:101–128, 1999.

-
- [30] M. A. Stremler and S. Basu. On point vortex models of exotic bluff body wakes. *Fluid Dynamics Research*, 46(6):061410, 2014.
 - [31] J. Vanneste. Vortex dynamics on a Möbius strip. *ArXiv preprint ArXiv:2102.07697*, 2021.